CENTRAL ASIAN JOURNAL OF MEDICAL AND NATURAL SCIENCES
https://cajmns.centralasianstudies.org/index.php/CAJMNS
Volume: 07 Issue: 04 | October 2026 ISSN: 2660-4159

Article

Synthesis and Characterization of Novel Maleimide and Phthalimide Derivatives: TGA Study and Antibacterial Activity Evaluation

Anaam Khalif Al-Azzawy*[1]

1. Salah Al-Din Education Directorate, Iraq
*Correspondence : anaam.k.athab@st.tu.edu.iq

Citation: Al-Azzawy A. K. Synthesis and Characterization of Novel Maleimide and Phthalimide Derivatives: TGA Study and Antibacterial Activity Evaluation. Central Asian Journal of Medical and Natural Science 2026, 7(4), 279-297.

Received: 10th May 2026
Revised: 11th Jun 2026
Accepted: 19th Jul 2026
Published: 28th Aug 2026

Abstract: A series of N-substituted maleimide and N-substituted phthalimide derivatives compounds (A5–A8) were prepared by means of a two-step synthetic pathway. First, the intermediate amic acids (A1-A4) were formed via ring-opening reactions of maleic anhydride and phthalic anhydride with primary amines, including 3,5-dimethoxyaniline and 2-amino-5-bromopyridine, in acetone at room temperature. In the second step, intermediate acids undergo ring-closure cyclization with anhydrous sodium acetate and acetic anhydride in thermal sublimation conditions for 4 h to afford final compounds in good yields. FT-IR,1H-NMR and 13C-NMR spectroscopy techniques were used to characterize the chemical structures of both intermediate and the final prepared compounds. The thermal stability of compounds A5 and A8 was studied by thermogravimetric analysis (TGA) under an inert argon atmosphere. The analysis of thermal curves indicated several stages of weight loss, correlated with the breakdown various functional groups in the structural framework and indicating excellent thermal stability of these compounds at high temperatures. Activity of compounds A5-A8 were assessed against two bacterial isolates (Gram-positive-Staphylococcus aureus , and Gram-negative-E.coli) by the diffusion method at 100%, 50%, and 25% concentrations. Results: Compared to the standard antibiotic gentamicin, the results displayed good repression of bacterial growth.

Keywords Maleimide, phthalimide, thermogravimetric analysis, biological activities.

1. Introduction

Heterocyclic compounds are cyclic organic compounds that have one or more heteroatoms in the ring, with nitrogen, oxygen, and sulphur the most common; their also well-known heterocyclic rings with other heteroatoms[1]. Carbocyclic compound is cyclic organic molecule that contains no other elements other than carbon in its ring. Heterocyclic compounds are considered one of the important classes of organic compounds used in various biological fields because they have proven to be effective against many diseases. The heterocyclic ring is a crucial skeleton structure of various biological active compounds such as DNA and RNA, chlorophyll, hemoglobin, vitamins and a lot more[2-4]. Pyrimidines are heterocyclic aromatic compounds that have nitrogen atoms at positions 1 and 3. They are symmetrical about one of the two to five axes[5]. Due to their diverse therapeutic applications and structural versatility, pyrimidine analogs have emerged as crucial scaffolds in medicinal chemistry. Pyrimidines, common constituents of numerous

bioactive and clinically approved drugs, serve as ideal scaffolds for the development of compounds with desired biological activity[6]. Pyrimidine derivatives are very important in the search for anticancer drugs because they can form hydrogen bonds and π-bonds and these compounds have similarities to nucleic acids. π interactions[7]. Halogens (F, Cl, Br, and I) are indispensable in the framework of modern-day drug development (particularly F and Cl). For instance, halogens are present in nearly 25% of approved drugs and 40% of lead molecules. Moreover, the most common drugs are also small molecules having halogen atoms[8]. Imides are heterocyclic compounds with an intact imide ring, and their general structure can be represented as –CO–N(R)–CO– where R is often substituted with an aryl or alkyl substituent. Imides possess structural features that yield potential biological activity and medicinal applications, they are hydrophobic, neutral compounds with the ability to traverse across cell membrane easily[9, 10]. The imido derivatives of phthalic acid are known as phthalimides. Therapeutic Effects of Current Imide Derivatives Their pharmacological activities and physiologically active features can be attributed to their imide ring and -CO-N(R)-CO- molecular structure. Phthalimides have gained considerable interest due to their anti-androgen receptor properties[11]. Phthalimide as a pharmacophore serves several functions in medicinal chemistry. Numerous phthalimides have been synthesized and investigated extensively in recent years with the purpose of targeting many diseases[12]. Phthalimide derivatives are reported to possess several pharmacological and biological activities including antimicrobial[13], anti-inflammatory[14], antifungal[15], antimalarial[16], and antioxidant[17]. This study involves the synthesis of new derivatives obtained by reacting aromatic and heterocyclic amines with phthalic acid and phthalic anhydride from modified maleimide and phthalimide. Furthermore, FT-IR, ^{1}H-NMR and ^{13}C-NMR spectroscopy have been utilized to confirm the chemical structures of the synthesized compounds and describe the results. The study also evaluates the thermal stability of those chemicals at high temperatures—through thermogravimetric analysis (TGA)—to understand their behavior under extreme circumstances. Finally, the biological activity of synthesized compounds as antibacterial agents is scrutinized paving grounds for their future therapeutic uses.

2. Materials and Methods

3,5-dimethoxyaniline, 5-bromopyrimidin-2-amine, maleic anhydride, phthalic anhydride, ethanol were purchased from Fluka and Aldrich; acetic anhydride and anhydrous sodium acetate were used as received. Melting points (uncorrected) of compounds were obtained using a melting point apparatus. FT-IR spectra were obtained using a Perkin-Elmer 1650 spectrometer (400-4000 cm^{-1}) in KBr disks. ^{1} H-NMR and ^{13} C-NMR spectra of a solution in dimethyl sulfoxide (DMSO-d_6) were recorded on Bruker spectroscopic ultra-shield magnets at a 300 MHz spectrometer using tetramethylsilane (TMS) as an internal standard. Thermal stability of some compounds was carried out via Simultaneous Differential Thermal Analysis and Thermo Gravimetric Analysis (SDT) Q600 Build 20. The bacterial isolates (*S.aureus* and *E. coli*) were provided by the Biological Activity department at the State Company for drug Industries and Medical Appliances(samarra- SDI).

Synthesis of amic acid (A_1-A_4)[18]

0.01mol of phthalic anhydride or maleic anhydride was disovelvinging 30 mL acetone in a 250 ml round-bottom flask. A solution of 0.01 mol (1.53 g) of 3,5-dimethoxyaniline or 0.01 mol (1.74 g) of 5-bromopyrimidin-2-amine dissolved in 20 mL acetone was added dropwise using a separating funnel to the liquid phase. The mixture was stirred at room temperature for 2 hr. The product was filtered out and recrystallized with ethanol. The physical properties of derivatives **A_1-A_4** are listed in Table 1.

Synthesis of N-substituted maleimide and phthalimide derivatives (A_5-A_8)[19]

A mixture of amic acid **(A_1-A_4)** (0.005 mol), acetic anhydride (20 mL), and anhydrous sodium acetate (0.164 g, 0.002 mol) was refluxed at 80 °C for 4 h. The resultant solution was cooled and poured into ice-cold water (100 mL). The precipitate was then filtered, washed several times with distilled water and recrystallized from ethanol to afford the pure imide derivatives **(A_5-A_8).** The physical properties of the synthesized derivatives are listed in Table 1.

Table 1. Physical Constants of Compounds (A_1-A_8)

Compound No.	Structure Formula	Molecular Formula	Molecular Weight(g/mol)	Color	M.P. ^{O}C	Yield %
A_1	(Z)-N-(3,5-dimethoxyphenyl)-4-(l1-oxidaneyl)-4-oxobut-2-enamide	$C_{12}H_{12}NO_5$	250.23	Light Yellow	220-222	68
A_2	2-((l1-oxidaneyl)carbonyl)-N-(3,5-dimethoxyphenyl)benzamide	$C_{16}H_{14}NO_5$	300.29	Yellow	235-237	71
A_3	(Z)-N-(5-bromopyrimidin-2-yl)-4-(l1-oxidaneyl)-4-oxobut-2-enamide	$C_8H_5BrN_3O_3$	271.05	Light Yellow	256-258	67
A_4	2-((l1-oxidaneyl)carbonyl)-N-(5-bromopyrimidin-2-yl)benzamide	$C_{12}H_7BrN_3O_3$	321.11	White	247-249	72
A_5	1-(3,5-dimethoxyphenyl)-1H-pyrrole-2,5-dione	$C_{12}H_{11}NO_4$	233.22	Pale	275-277	68%
A_6	2-(3,5-dimethoxyphenyl)isoindoline-1,3-dione	$C_{16}H_{13}NO_4$	283.28	Off White	264-266	72%
A_7	2-(5-bromopyrimidin-2-yl)isoindoline-1,3-dione	$C_8H_4BrN_3O_2$	254.04	White	267-269	64%
A_8	2-(5-bromopyrimidin-2-yl)isoindoline-1,3-dione	$C_{12}H_6BrN_3O_2$	304.10	Yellow	237-239	71%

3. Results and discussion

The **A_1-A_8** compounds were synthesized in two steps, where stage 1: Primary amines (3,5-dimethoxyaniline and 5-bromopyrimidin-2-amine) were treated with phthalic anhydride or maleic anhydride in acetone to provide amic acids as intermediates. Stage 2: The obtained amic acids were ring-closed (cyclized) through dehydration with acetic anhydride and anhydrous sodium acetate at a temperature of 80°C during a period of 4 hours. as shown in Scheme 1.

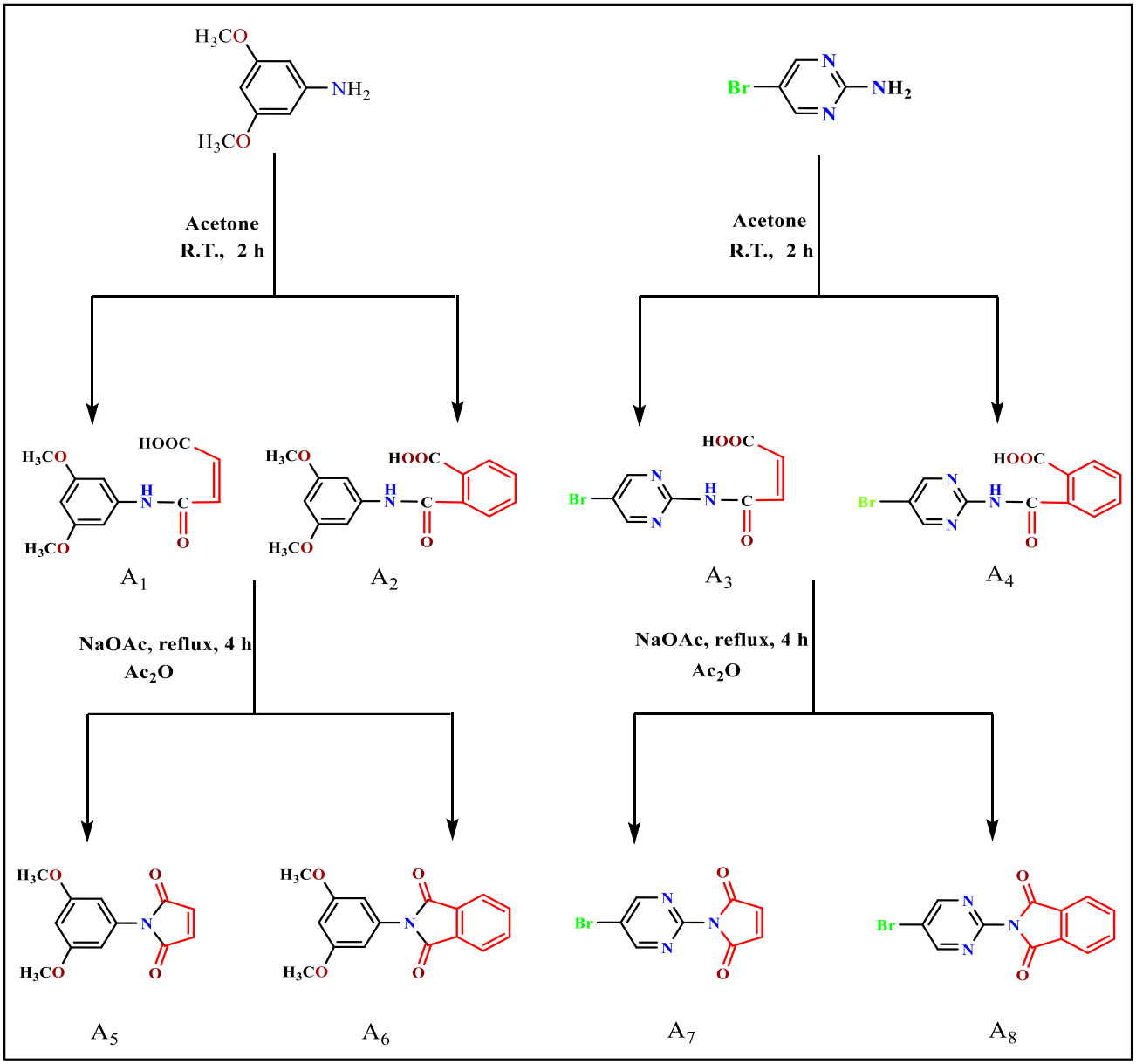

Scheme 1. Synthesis of *N*-Substituted maleimide and phthalimide derivatives **(A1-A8)**.

Characterization of N-Substituted Maleimide and Phthalimide Derivatives (A1-A8)

Maleimide and phthalimide derivatives **(A1-A8)** were synthesized in acetone from equimolar amounts of primary amine derivatives with phthalic anhydride and maleic anhydride, respectively. As shown in Scheme 2, the mechanism of this reaction involves attack of the amine on the carbonyl carbon of anhydride with scission of the ring, internal rotation and loss of water to yield the final product[20].

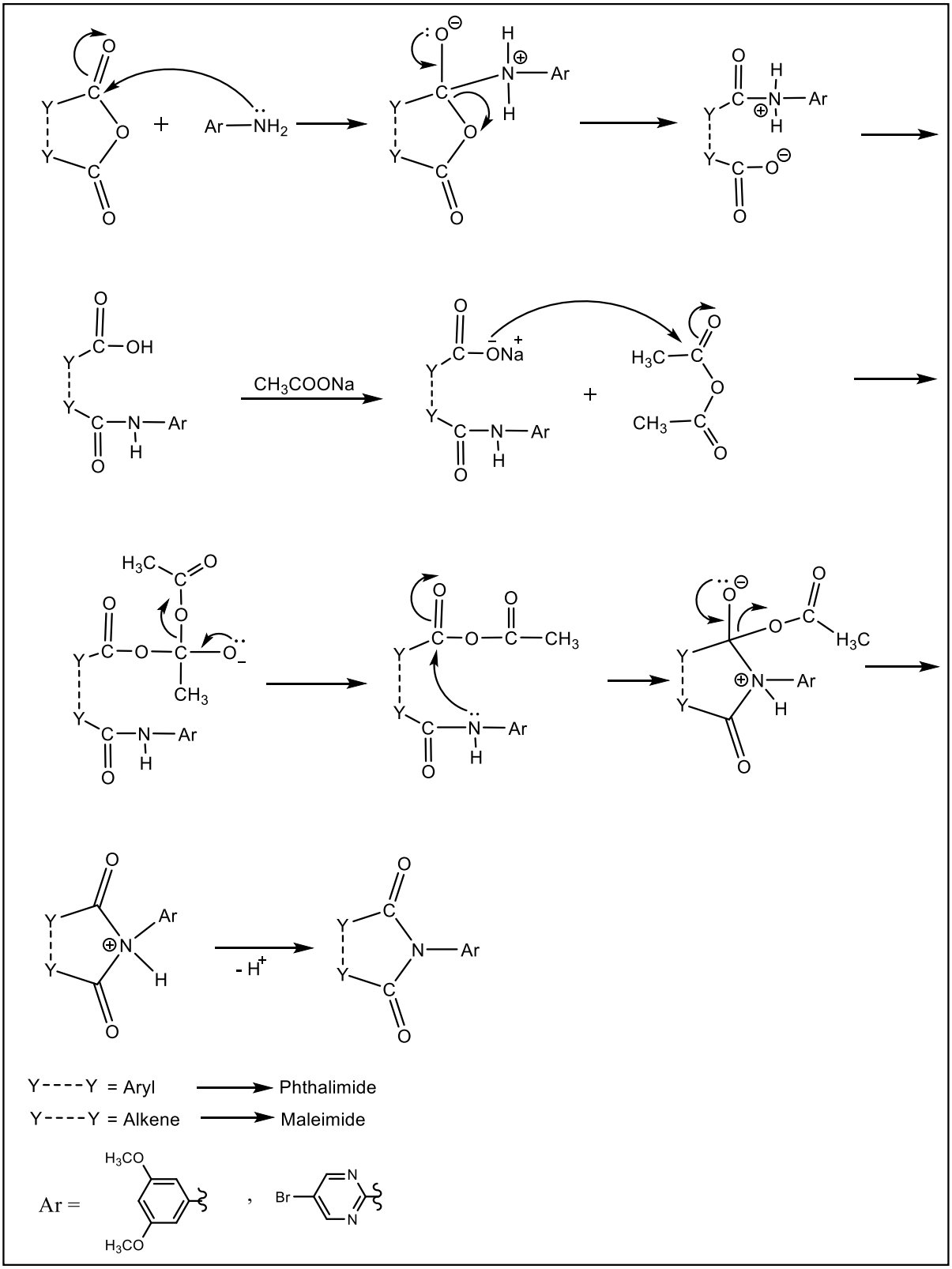

FT-IR **Scheme 2.** The mechanism of preparation of compounds (A_1-A_8)

The compound **(A_1)** was characterized by spectral methods. The N-H bond stretch of the amide group is indicated by a band in the NIIR FT-IR spectrum (frequency = 3377 cm^{-1})[21]. At position (2500-3350) cm^{-1}, an absorption band was formed[22]. associated with the (O-H) carboxyl group bond stretching. The carbonyl of carboxylic acid was observed as a sharp and strong peak at 1720 cm^{-1}, while a band in the 1674 cm^{-1} area could be attributed to C=O amide bond stretching[23]. See Figure **1.**

FT-IR Spectrum of compound **(A_4)** exhibited a band due to the N-H bond stretch of the amide group at frequency 3322 cm^{-1}. A broad absorption band at (2800-3300) cm^{-1}, assigned to the (O-H) carboxyl group bond stretch. An intense, strong band was also detected at 1724 cm^{-1} for the carbonyl of carboxylic acid and another band was seen at 1688 cm-1 more property to C=O amide bond stretch. See Figure 2.

The FT-IR spectra of compound **(A_5)** displayed two absorption bands in the range of 1780 cm^{-1} and 1730 cm^{-1}[24, 25]. and (b) represented the symmetrical and asymmetric stretching vibratioins of imide carbonyl group (C=O), respectively. The aromatic (C-H) stretching gives rise to the absorption band at 3019 cm^{-1}, while its counterpart for the aliphatic region appears (2986, 2866) cm^{-1} and an absorption band is observed at 1256 cm^{-1} attributed to stretching of (C-N) bond. See Figure 3.

The FT-IR spectrum of compound **(A_8)** display two characteristic absorption bands at 1782 cm^{-1} and 1694 cm^{-1}, attributable for the symmetrical and asymmetric stretching vibratioins of the imide carbonyl group (C=O)[26]. respectively. The absorbtion band observed at 3082 cm^{-1} is assigned to the aromatic (C-H) stretching, and the bands appeared at (1283) cm^{-1} are due to the stretching of the (C-N) bond[27]. See Figure 4. Absorption bands of the prepared compounds are presented in Table 2.

Table 2. spectral data of the prepared compounds (A_1-A_8).

Compound No.	υ N-H amide	υ O-H carboxylic	υ C-H Aromatic	υ C=O acid	υ C=O amide Imide	υ C=C Alkenyl	Other absorptions
A_1	3377	2500-3350	3070	1720	1674 -	1597	υ C-H 2945. 2860
A_2	3415	2500-3250	3067	1722	1665 -	-	υ C-H 2972. 2837
A_3	3372	2600-3150	3058	1718	1672 -	1634	υ C-Br 1067
A_4	3322	2800-3300	3177	1724	1688 -	-	υ C-Br 1095
A_5	-	-	3019	-	1780 1730	1670	υ C-H 2986. 2866
A_6	-	-	3073	-	1763 1715	-	υ C-H 2967. 2838
A_7	-	-	3073		1756 1712	1645	υ C-Br 1057
A_8	-	-	3082		1782 1694	-	υ C-Br 1026

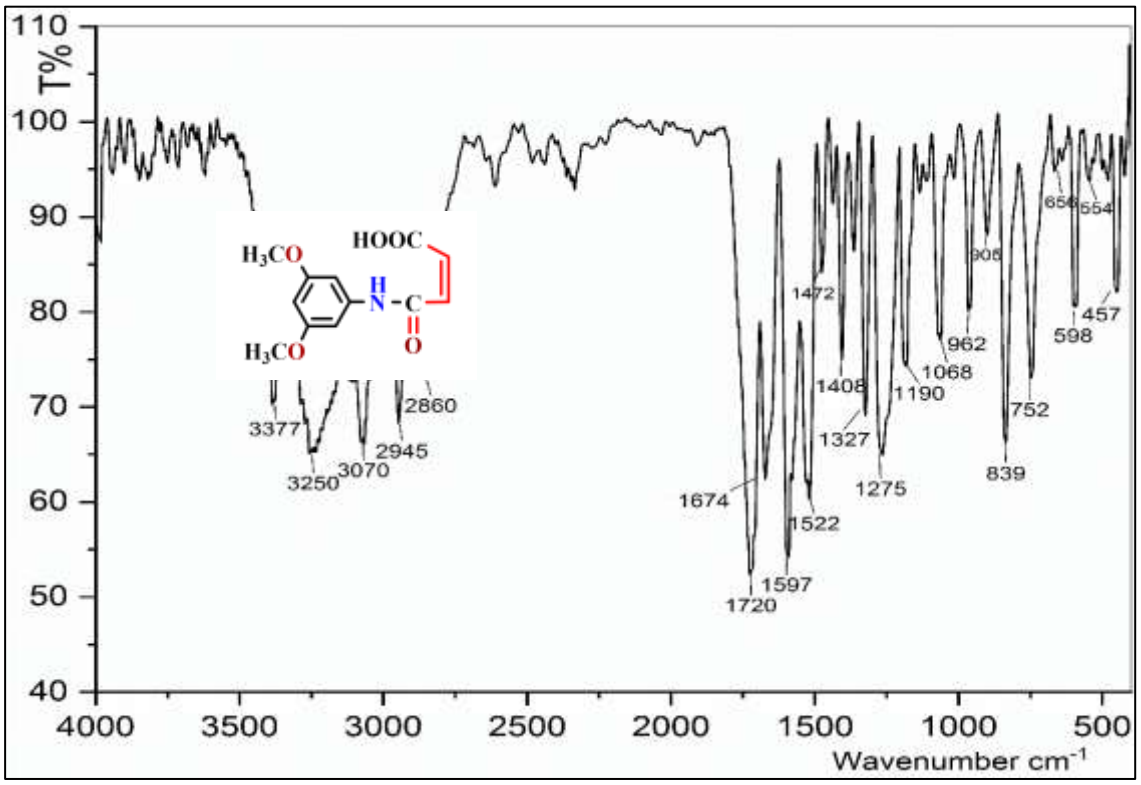

Figure 1. FT-IR spectrum of compounds (A_1).

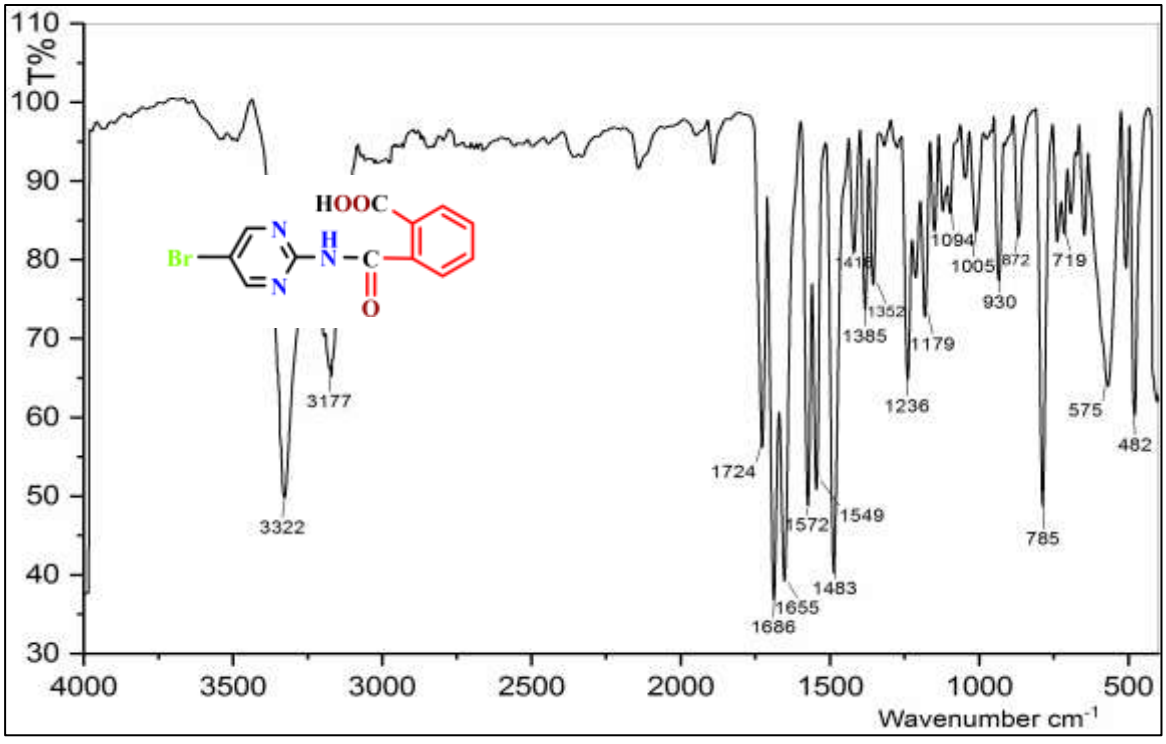

Figure 2. FT-IR spectrum of compounds. (A_4).

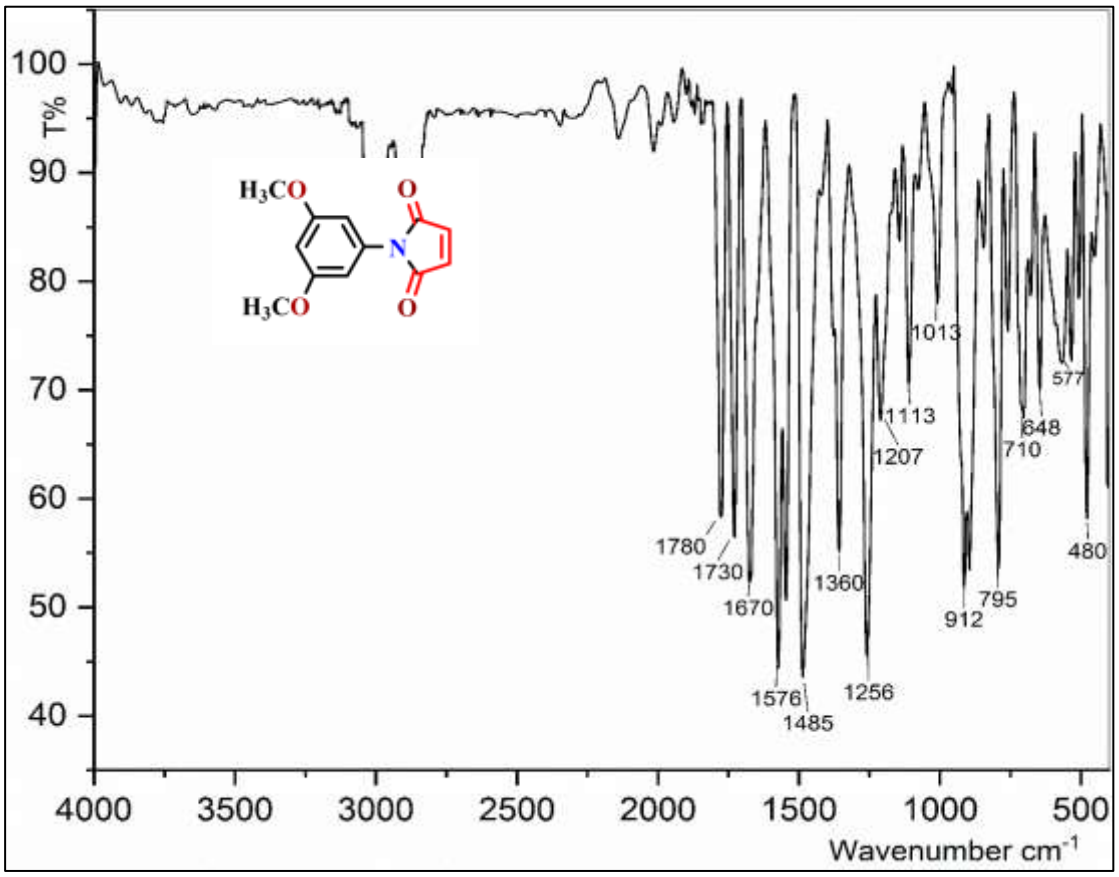

Figure 3. FT-IR spectrum of compounds (A_5).

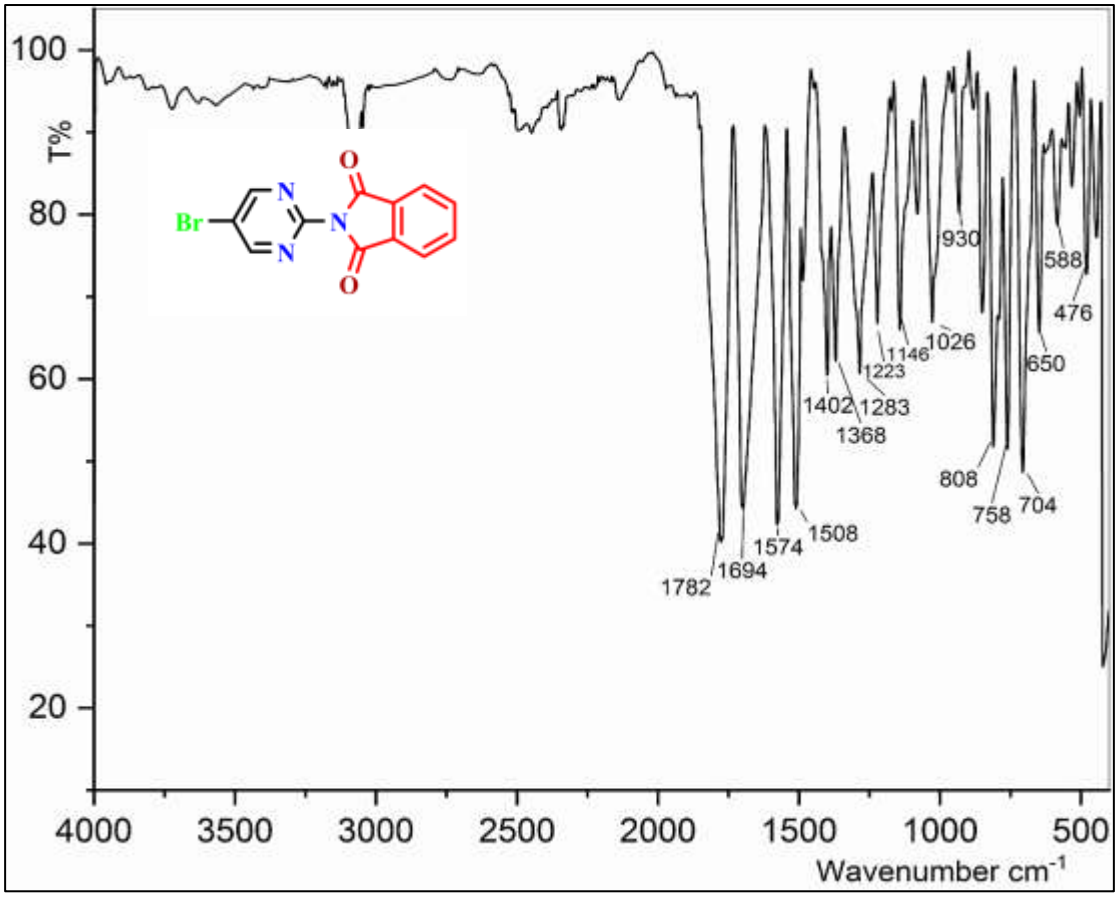

Figure 4. FT-IR spectrum of compounds (A_8).

^{1}H-NMR and ^{13}C-NMR Spectra Analysis

Its ^{1}H-NMR of compound **(A_1)** showed a singlet at δ= 3.46 ppm corresponding to methoxy protons (OCH_3) and another singlet at δ= 10.68 ppm related with the amide proton (CO-NH)[28]. The carboxyl hydroxyl proton (OH) appeared at δ= 13.10 ppm[29]. In addition, several signals within the range (7.58–7.98) ppm correspond to aromatic protons. DMSO-d_6 solvent signals appeared at δ= (2.50-2.51) ppm, as shown in Fig. 5. The ^{1}H-NMR spectrum of compound **(A_4)** exhibited a singlet at δ= 10.69 ppm that was assigned to the amide proton (CO-NH-), and another singlet at δ= 13.10 ppm corresponding to the carboxyl hydroxyl proton (OH). In addition, several peaks between δ= (7.69–7.95) ppm correspond to the aromatic protons. The signals for the solvent (DMSO-d_6) were noticed at δ= (2.49–2.51) ppm, shown in Figure 6. ^{1}H-NMR spectrum of compound **(A_5)** showed singlet at δ= 2.62-3.23 ppm due to methoxy protons (OCH_3), and a few multiple signals in range (7.63–8.10) ppm corresponding with aromatic protons. Figure 7 showed the solvent (DMSO-d6) signals at δ= (2.49) ppm. In the ^{1}H-NMR spectrum of compound **(A_8)**, multiple signals appeared at (7.91–8.36) ppm due to aromatic protons. Figure 8 shows the solvent (DMSO-d_6) signals appeared at δ= (2.57) pp.

The ^{13}C-NMR spectrum of compound **A_1** (Figure 9) shows two chemical shifts at δ= 169.27 ppm and δ =163.21 ppm for the two carbonyl carbons of the amide and carboxy groups respectively In the aromatic region[30], the signal at δ= 154.39 ppm corresponds to the carbons bound to methoxy groups. The respective signals for the sp^2 carbons (aromatic and alkenic (C=C))were located in the δ= 130.98–137.23 ppm range. Similarly, ortho carbons gave a peak at δ = 110.51 ppm. The last signal for the methoxy carbons appeared at 64.37 ppm and the solvent (DMSO-d_6) signal at 39.52 ppm.

Identification of Compound **(A_5)** by ^{13}C-NMR spectroscopy. The two carbonyl groups (C=O) of phthalimide ring appeared at δ= 169.27 ppm[31]; the signal at δ= 163.27 ppm is assigned to the aromatic carbons connected to methoxy group. Nevertheless, the two carbon atoms that constitute the double bond in the maleimide ring retained a signal within δ= 130-135 ppm, along with their other aromatic carbon atoms. The chemical shift for the two methoxy groups (OCH_3) was observed at δ 53.56 ppm. The signal position at δ= 78.38 ppm was assigned for the methine group (CH) of the δ= 3,5-dimethoxyphenyl ring and a solvent signal emerged at δ= 38–40 ppm. Note Figure 10.

Compound **(A_8)** gave a sharp signal in the ^{13}C-NMR spectrum at δ= 170 ppmwhich is assignable to carbon N=C-N of pyrimidine ring. a signal appeared at δ= 158 ppm for the C=N carbon in the same ring, and another appeared at δ= 166 ppm for the carbonyl carbon of phthalimide ring. The rest of the aromatic carbon all exhibited resonances between δ= (113-135) ppm. See Figure 11.

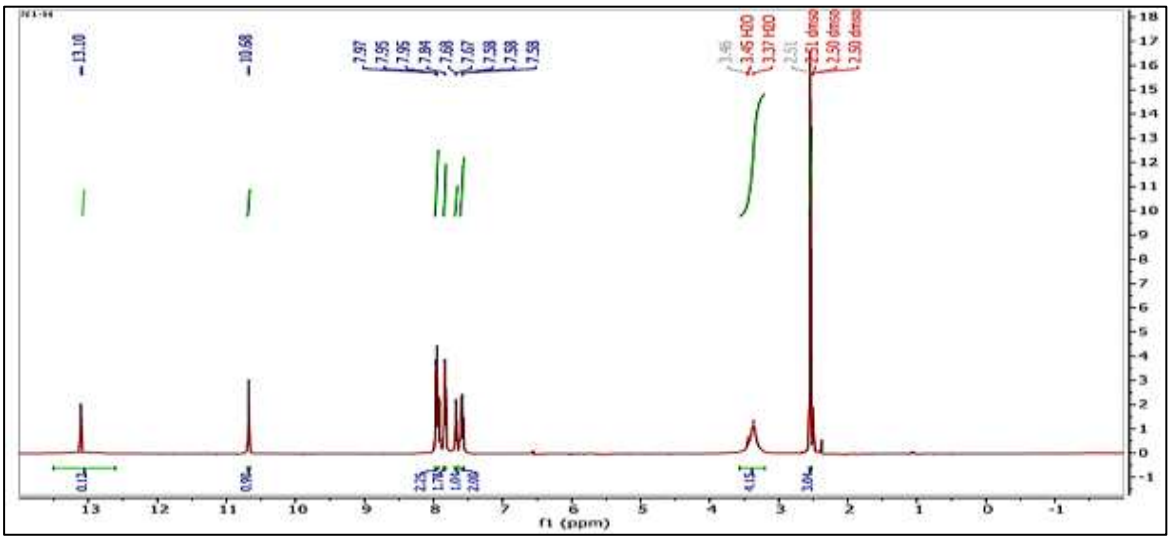

Figure 5. [1]H-NMR spectrum of compounds (A_1).

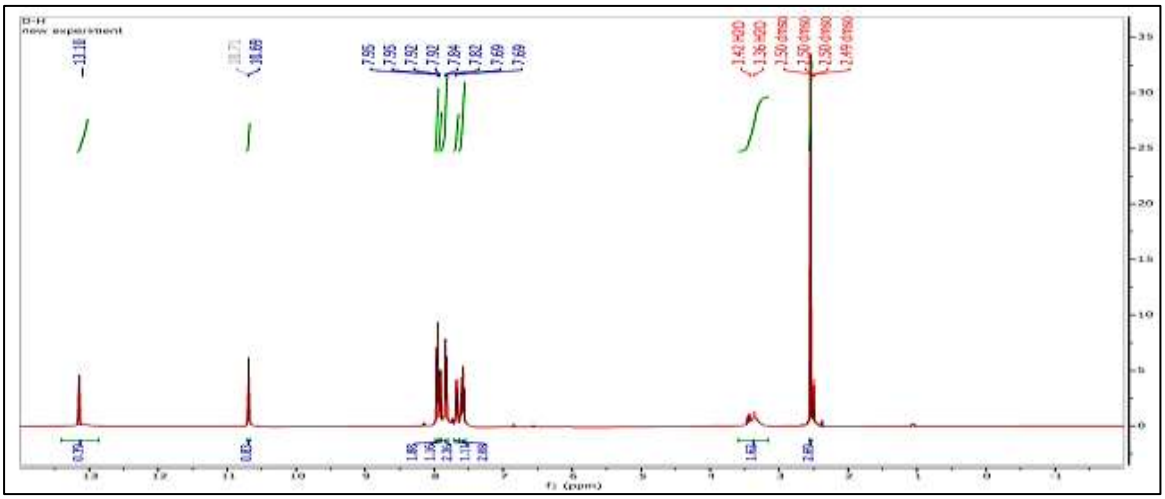

Figure 6: [1]H-NMR spectrum of compounds (A_4).

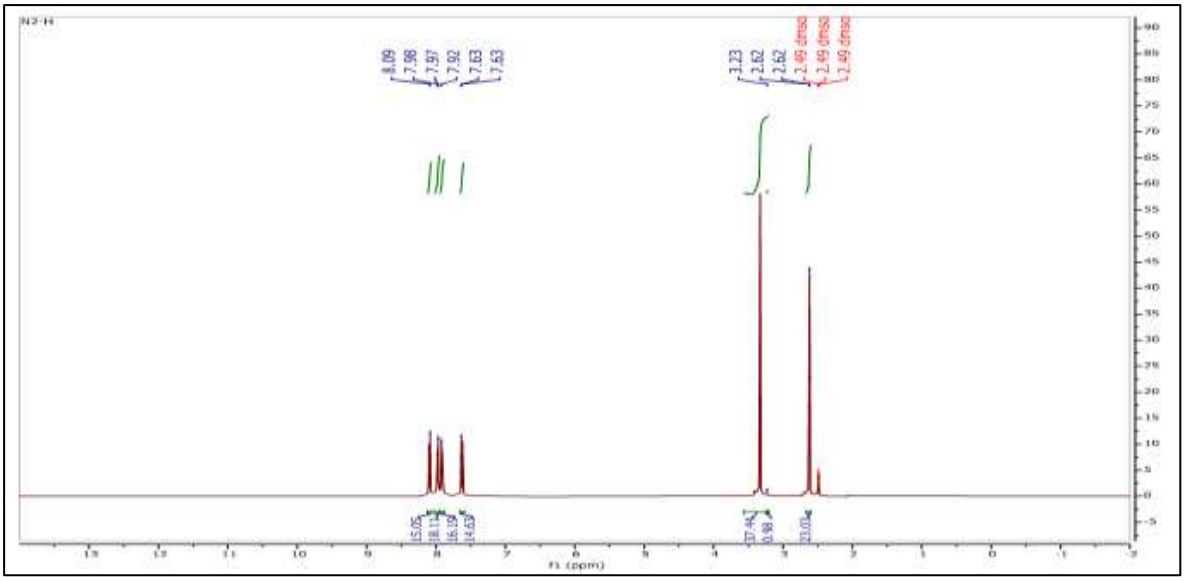

Figure 7: [1]H-NMR spectrum of compounds (A_5).

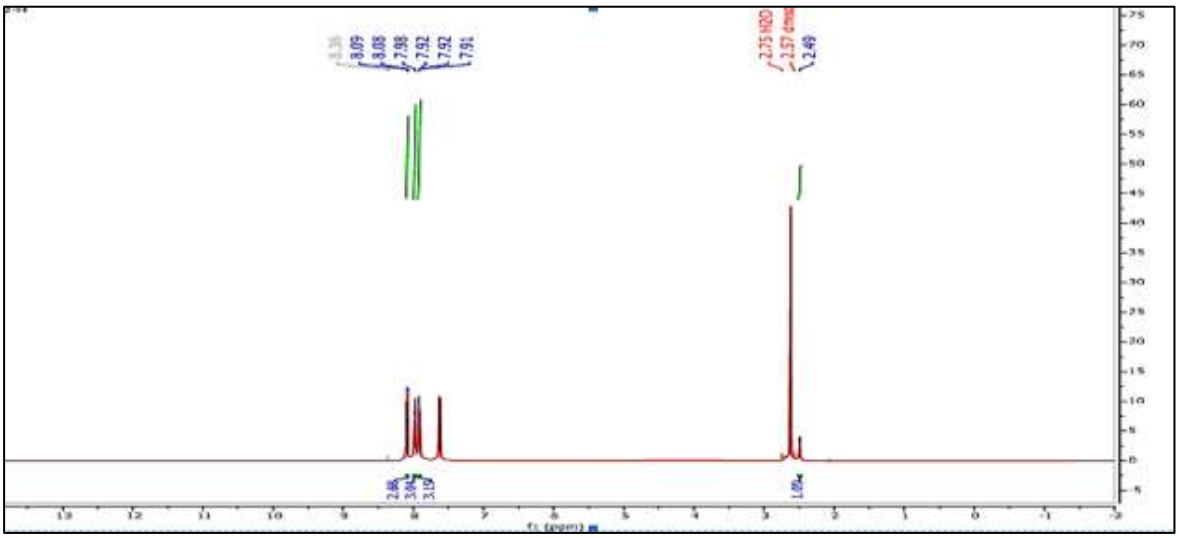

Figure 7. [1]H-NMR spectrum of compounds (A_8).

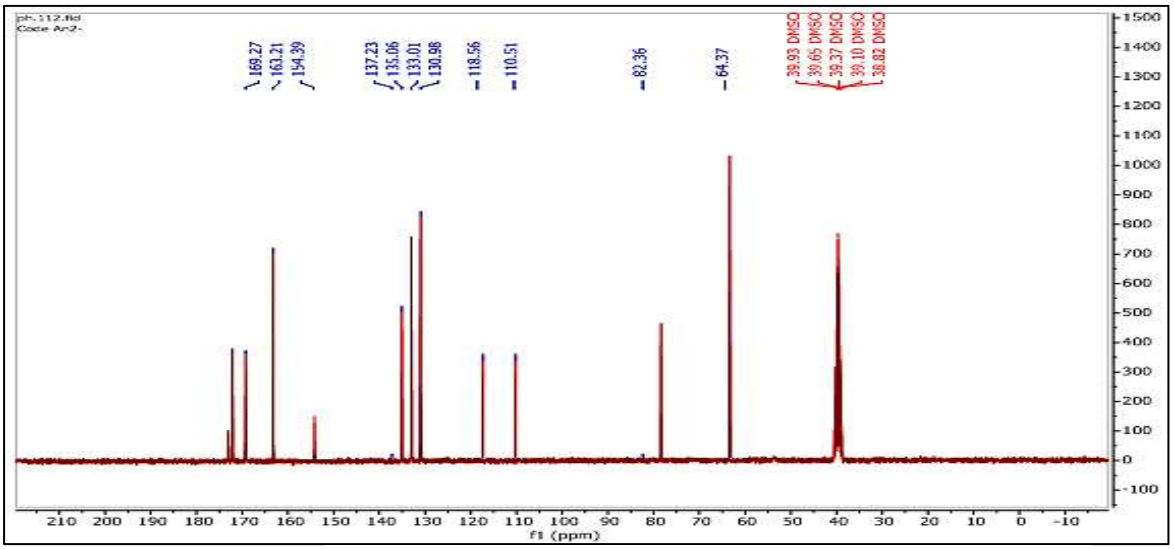

Figure 9. [13]C-NMR spectrum of compounds (A_1).

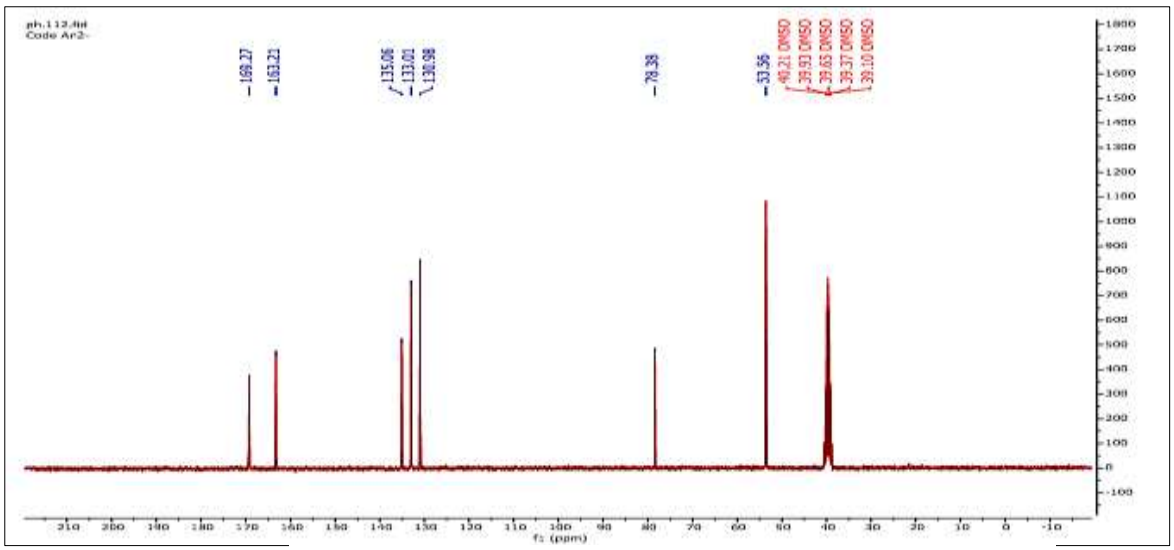

Figure 10. [13]C-NMR spectrum of compounds (A_5).

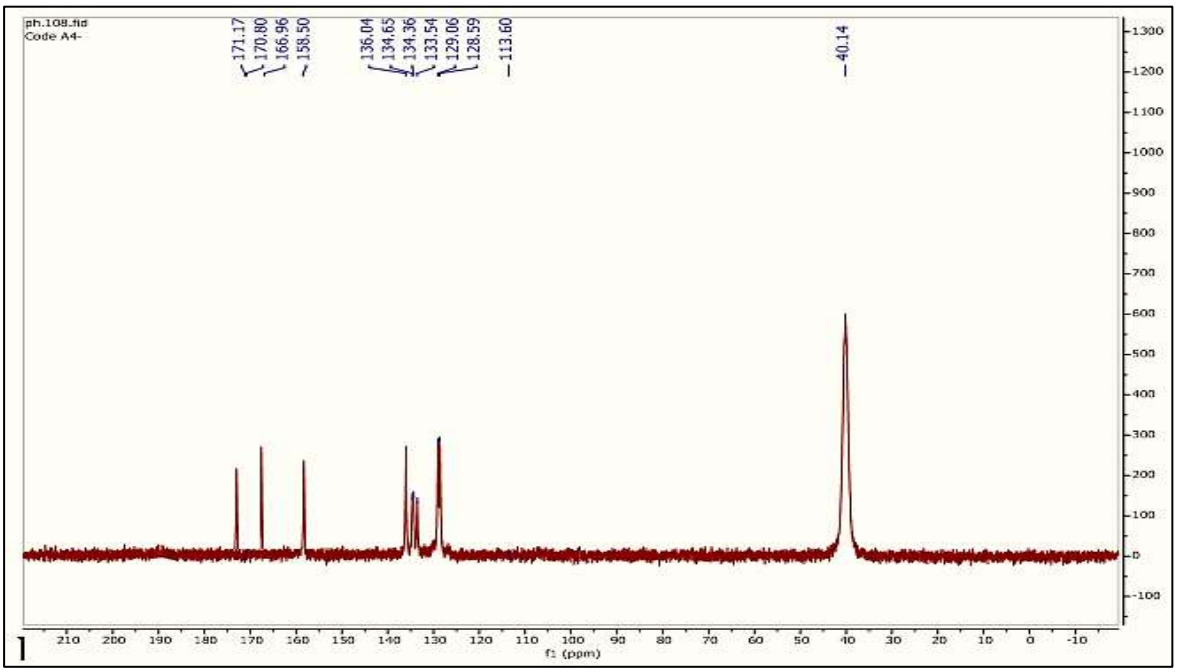

Figure 11. ^{13}C-NMR spectrum of compounds (A_8).

Thermogravimetric Analysis (TGA)

The thermal stabilities of prepared compounds **A**$_5$ and **A**$_8$ and it indicated whether water were present in structures or not were evaluated by thermogravimetric (TG) analysis. The measurements were carried out in argon atmosphere with heating rates of 20°C per minute. The thermal decomposition curves of **A**$_5$ and **A**$_8$ are demonstrated in Figures 12 and 13, respectively. In this case, the weight (wt%) of the sample was determined at the temperature increase (25-800 °C) under argon (Ar) gas atmosphere. The weight loss occurred in three stages because of the degradation of the compounds.

The TGA (thermogravimetric decomposition) curve of compound **A**$_5$ (Figure 12) indicates that the compound loses weight through multistage. The first thing to stand out is that, in addition to the compound has a total weight loss of 83.18%, there are four main stages of weight loss for the compound (in weight loss %). Stage one is between 25–100°C The percentage loss is 6.365% (0.1738 mg) and is due to the presence of moisture or solvent molecules (for example, chloroform) released during preparation. Phase II: At 100-200 °C, the losses correspond to 42.86% (1.170 mg) Such a decomposition corresponds to the breaking of the maleimide ring and dissociation of the substituted benzene ring. This relatively high percentage suggests that the functional region of the compound will be the first to respond to heat.

The loss rate is 9.005 % (0.245 mg), which indicates the loss of two methoxy groups OCH_3 or small molecules caused by dissociating the remaining bonds in the third stage (200–330 °C). The fourth stage indicates a temperature range of 330–450 °C combining a weight loss of 9.985% (0.2726 mg), which may correspond to further destruction of benzene ring and emission of products such as CO or C_2H_2. This led to a delay stage at 450–800 °C, which brought about a 14.96% (0.4086 mg) weight loss. In this case, the residual carbon backbone in the benzene ring breaks down, leaving the material as a more inert solid carbon section. The overall loss in weight at 800 °C is 83.13%, which represents the final product. Argon gas does not decompose the rest ash which is around 16.82% of the total weight that is thermally stable carbonaceous ash. From this, we can infer that this compound was thermally stable until 100°C, above which this compound does start to decompose, so we know the bond with the maleimide ring and the benzene ring is heat-sensitive. That implies that the compound would not be viable for applications needing

high-temp processing, for instance, polymers processed over 140 ℃. Multiple stages of decomposition signifies the disparity in bond energy in relation to breaking different bonds in the molecule. Accordingly, the safe temperature of this compound is no higher than 100 ℃ because above this temperature, this compound undergoes a chemical reaction due to heating, causing its properties to be lost. Nevertheless, the carbon residue at 800°C of 16.82% for this compound shows that the compound is fairly efficient in producing a thermally stabilized carbon layer, allowing for the investigation of its characteristics in a fire-resistant material or as an advanced carbon material.

The TGA curve of compound **A**$_8$ is summarized in Fig. 13, and the TGA curve can be divided into three ranges with the sum of weight percentages is equal to 99.77%. Stage 1: 100–300°C temperature range: 79.70% (7.532 mg) lost. As demonstrated by their high loss rate, the main structure (phthalimide ring and pyrimidine ring) and carbonyl groups of the compound must be destroyed, leaving only simple carbon residues or heavy atoms. The second component of the loss of mass in the range of 300–550 °C was equal to 12.10% (1.144 mg), which was due to the volatilization of parts of the carbon chain along with the bromine atom. Stage three, 550–800°C, 7.962% (0.7524 mg) was lost, which is likely related to the volatization or oxidation of the final residues of carbon. The yield loss of 0.23% at 800 °C corresponds to the presence of very few carbon residues. The result from decomposition, we can also see that the compound is nicely stable until 130°C, and then starts to decompose fairly fast. In addition, absence of weight losses prior to 100°C shows that the compound is hydrophilic and not have any bound water molecules. The almost 100% rate of weight loss, also indicates the compound is wholly organic and contains no minerals.

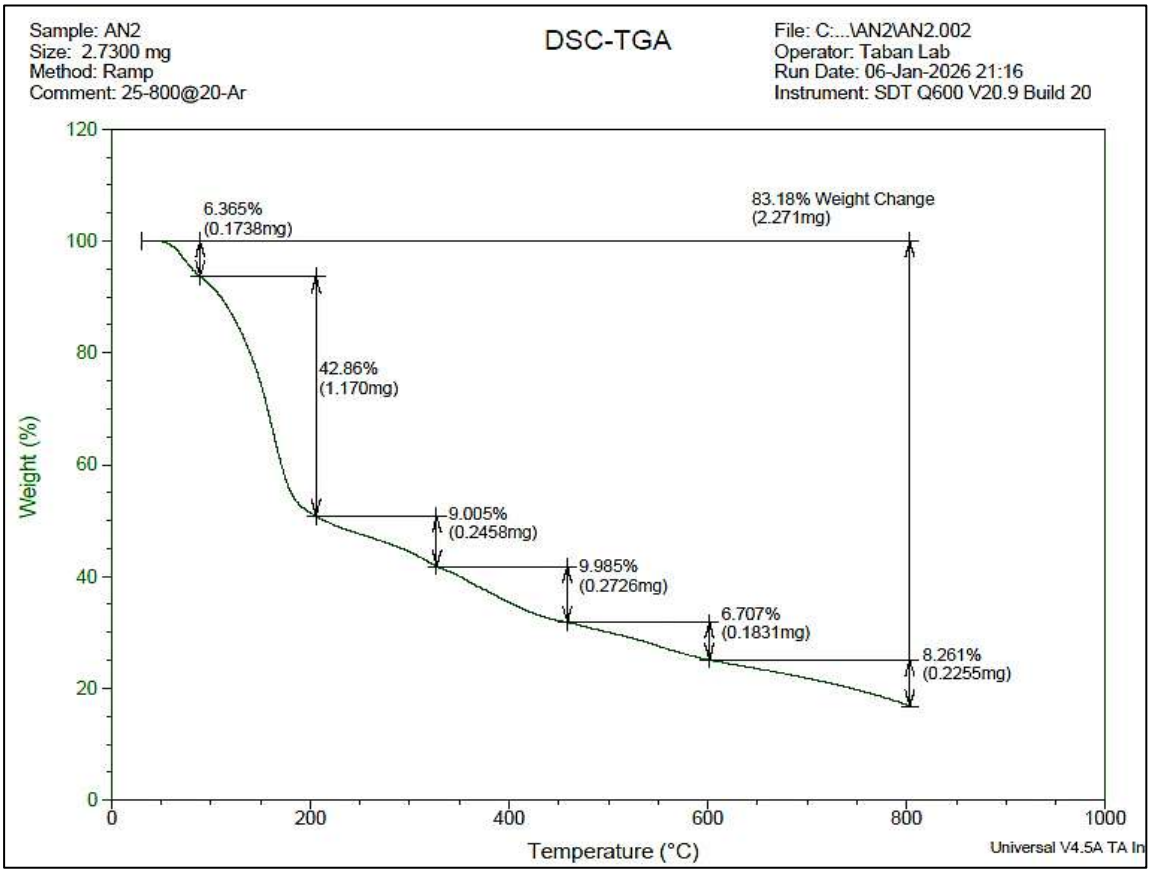

Figure 12. (TGA) curve of compound (A$_5$).

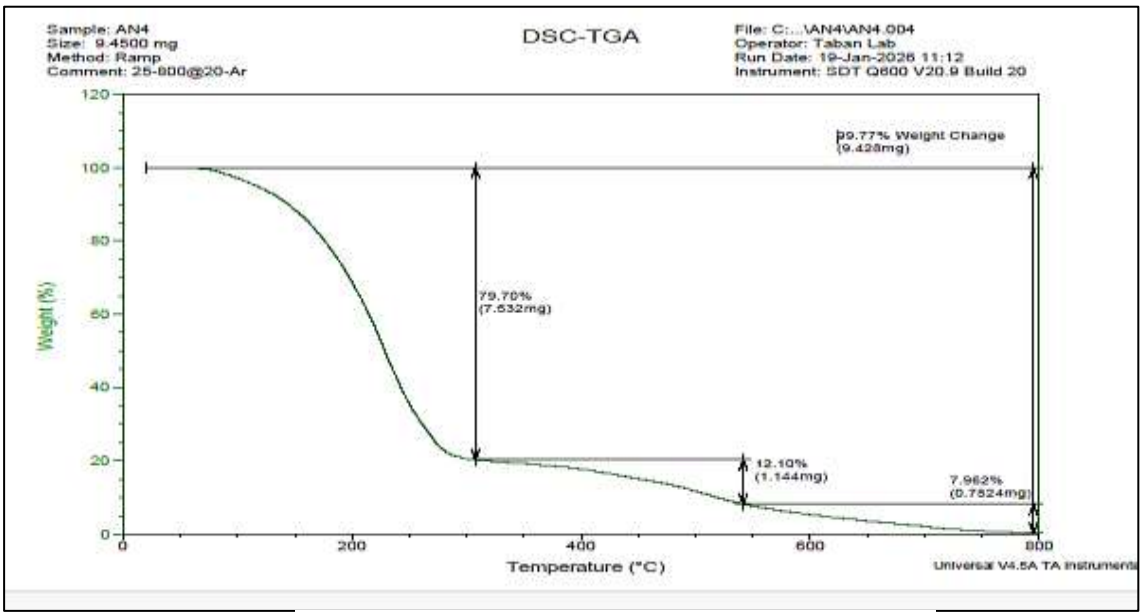

Figure 13. (TGA) curve of compound (A_8).

Antibacterial activity assessment

The synthesized compounds **(A_5, A_6, A_7, and A_8)** were screened for their antibacterial activity against two strains of bacteria (*Staphylococcus aureus* and *Escherichia coli*). Each concentration (25%, 50%, and 100%) of the compounds dissolved in DMSO was tested. According to USP33, the cylinder-plate method[32]. was then used with the application of medium 1. The suspension obtained from the bacterial isolates was activated at 37℃ for 24 hours and then added to the plate and incubated for another 24 hours. Inhibition zones were then measured to demonstrate the effectiveness of the respective concentrations. The antibacterial activity was assessed based on the diameter of the inhibition zone (IZD, mm) and compared with the antibiotic[33]. The compounds were found to be potent and consistent inhibitors of S. aureus growth with inhibition zones ranging between 15.5 mm and 16.7 mm at 100% concentration. This shows that due to their reactive functional groups, the synthesized compounds have the potential to penetrate the cell wall of Gram-positive bacteria. Results also confirmed the potency of compound **A_5** against S. aureus, which exhibited the largest inhibition zone of 16.7 mm, followed at 100% concentration by the antibiotic gentamicin (15.5 mm). A stepwise increase in the inhibition effect was observed for these compounds, whereas compound **A_5** had 25% more pronounced inhibition (16.4 mm) than 50% (13.9 mm), possibly suggesting some specific dispersion properties of the compounds in the culture medium. The affinity for gentamicin was observed for all compounds at 100% concentration, which makes them appropriate candidates as antibacterial agents against Gram-positive bacteria. In terms of the anti-Gram-negative Escherichia coli efficacy of the screened compounds, the compound displayed a significant efficacy of 25%, with 15.7 mm which was nearly similar to the value of the standard antibiotic at 15.6 mm. Compound **A_7** achieved stable efficacy at 100% and 50% concentrations (13.3 mm), but levels are lower than those of standard antibiotic. The close similarity in diameters of inhibition suggests that the structural framework of these compounds is highly stable in the culture medium. These results represent early and encouraging intermediates for defining how these compounds work inside the bacterial cell in future studies. See Figures 14-17.

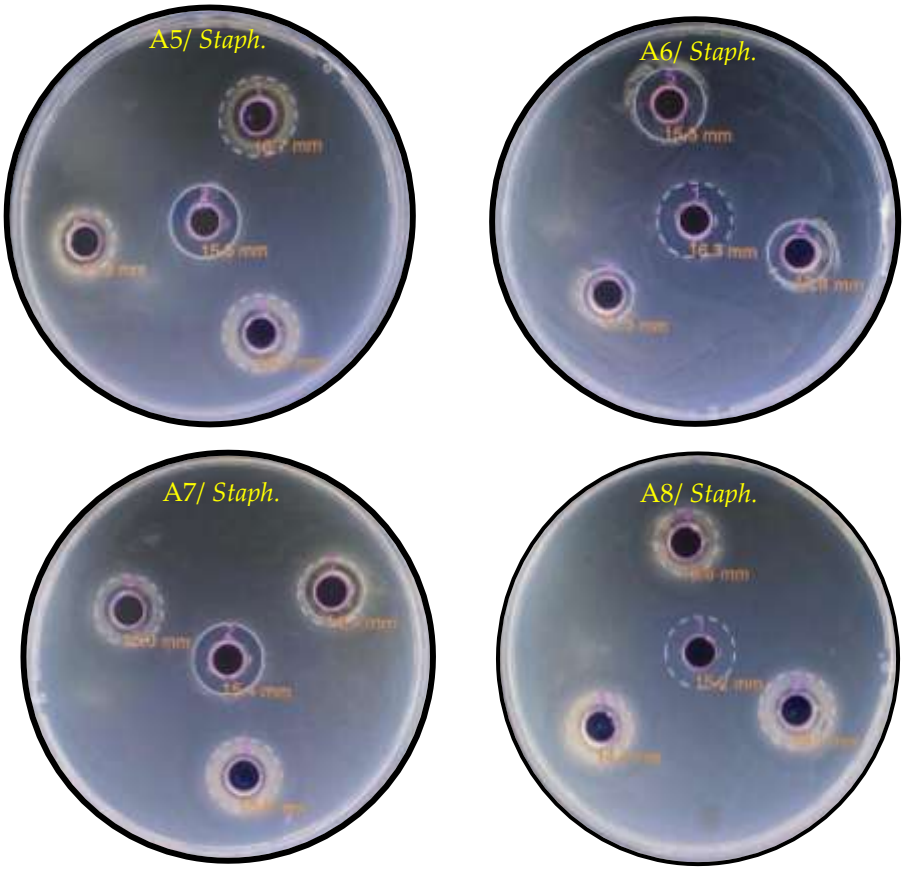

Figure 14. Bacterial activity of the compounds against Staphylococcus aureus bacteria

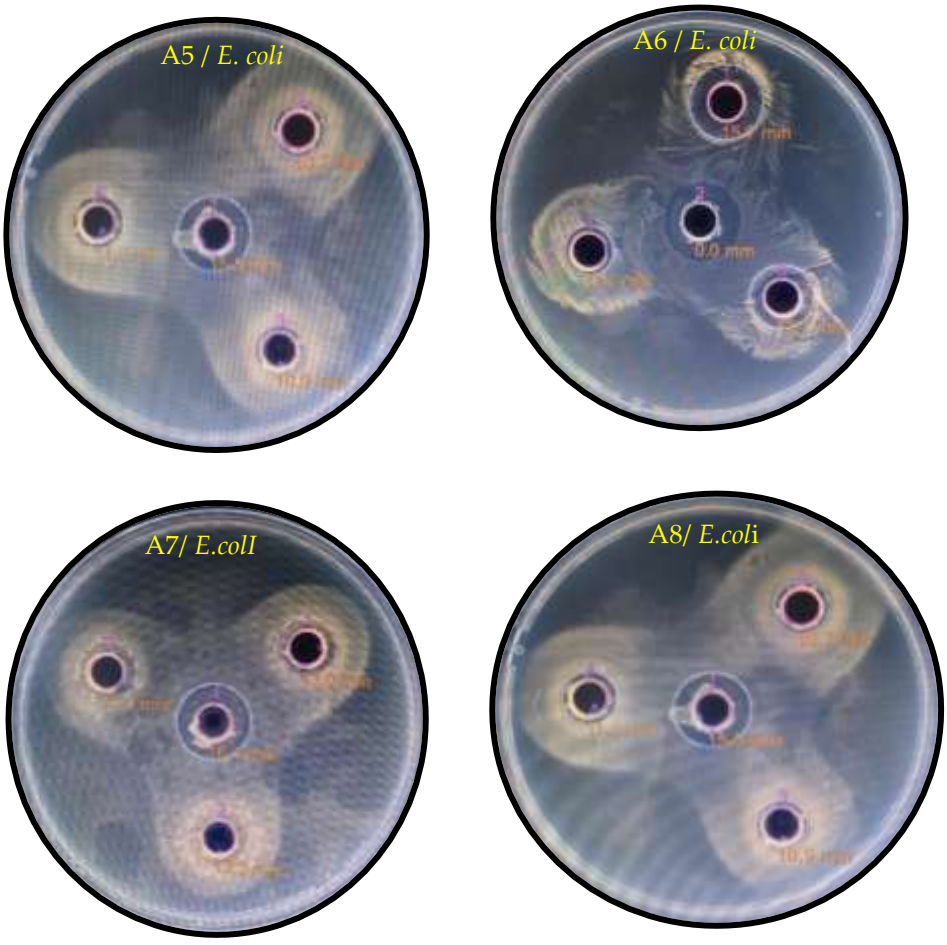

Figure 15. Bacterial activity of the compounds against *E. coli* bacteria

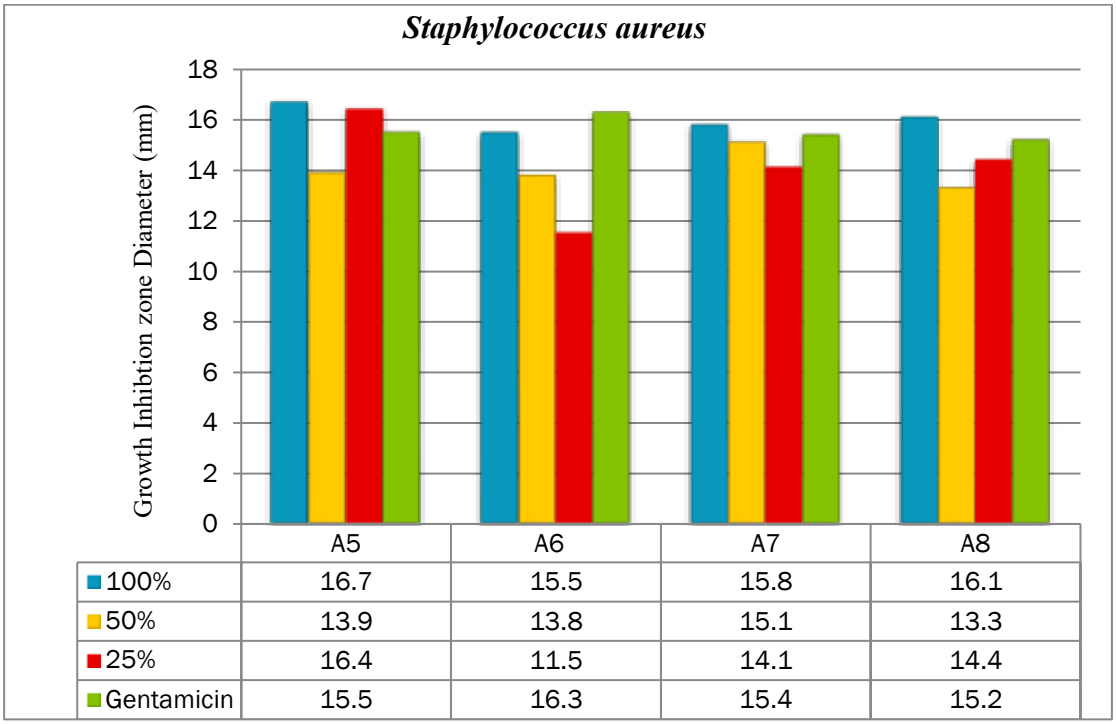

	A5	A6	A7	A8
100%	16.7	15.5	15.8	16.1
50%	13.9	13.8	15.1	13.3
25%	16.4	11.5	14.1	14.4
Gentamicin	15.5	16.3	15.4	15.2

Figure 16. Effect of different concentrations on the growth of *S. aureus* bacterial.

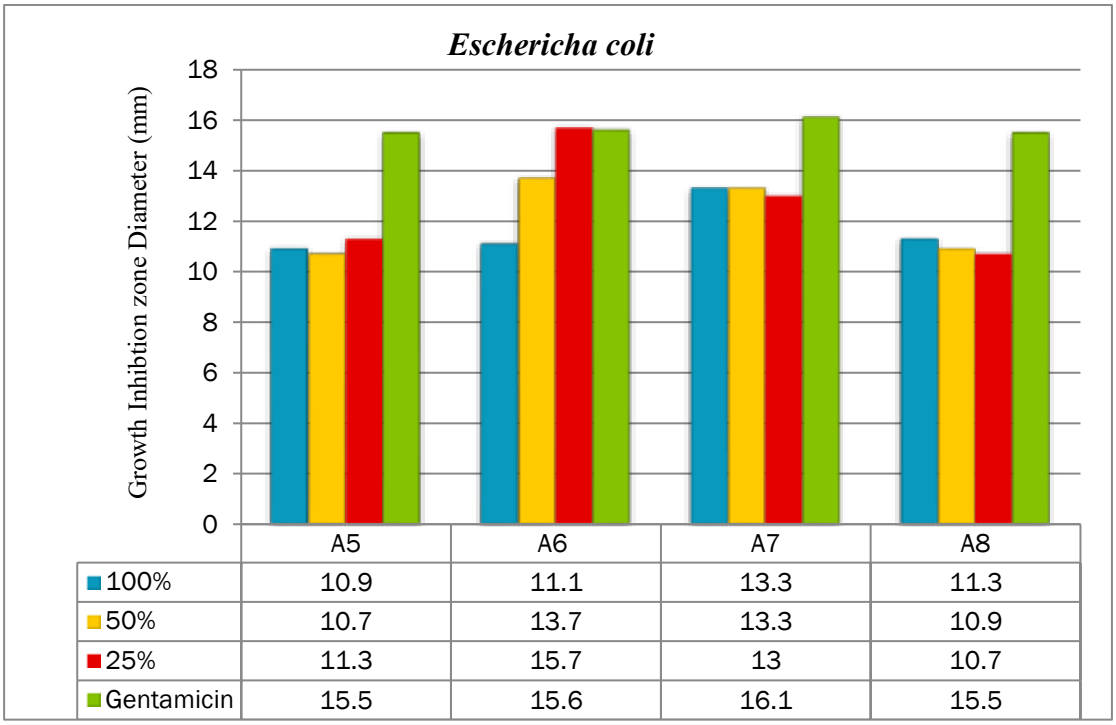

	A5	A6	A7	A8
100%	10.9	11.1	13.3	11.3
50%	10.7	13.7	13.3	10.9
25%	11.3	15.7	13	10.7
Gentamicin	15.5	15.6	16.1	15.5

Figure 17. Effect of different concentrations on the growth of *E. coli* bacterial.

4. Conclusion

A new series of maleimide and phthalimide derivatives **(A_5-A_8)** were achieved through a 2-step rection path as indicated by the subsequent formation of amic acids as intermeidate compounds, that were then cyclized under thermal sublimation conditions in the presence of anhydrous sodium acetate and acetic anhydride, leading to a completion of hithhly eeffecient behavior of this reaction to offer good end products and yield ratios. Spectral characterization results assured structure shapes of the synthesized compounds as FT-IR results showed that the characteristic bands for amide and carboxylic acid groups

had disappeared after modification and strong absorptions of the carbonyl groups had appeared. The ^{1}H-NMR and ^{13}C-NMR spectra also consistently showed signals at the positions theoretically expected which confirmed the structural design of the prepared compounds. Results from thermal analysis (Figure 5) showed outstanding stability of the compounds **(A_5-A_8)** up to 130 °C; no evidence of moisture or of the presence of bound water molecules was recorded, as no loss of weight preceded 100 °C, and all four compounds reveal a unique pathway of decomposition, the total loss at elevated temperatures approaching ca. ~100%, indicating their purely organic nature, confirming the regularity of chemical composition and the effectiveness of the preparation. The inhibition zone showed very good inhibition of all the prepared compounds against *S. aureus* bacteria, in which the compound **A_5** achieved an inhibition zone of 16.7 mm at a concentration of 100%, as compared to 15.5 mm for the standard antibiotic gentamicin. The results also illustrated that prepared compounds had inhibitory activity against *E. coli*, a bacterium, with a diameter of inhibition zone 15.7 mm for **A_6** at 25%, and this is a value that is very close to the ability of the gentamicin standard, 15.6 mm. The results of the biological activity showed that the compounds prepared acted as an effective antibacterial agent with a wide antibacterial spectrum as compared to gentamicin and have also revealed a different response to *E. coli* and *S. aureus* bacteria due to a difference in the properties of the cell wall.

REFERENCES

[1] C. Mallappa, M. Chahar, N. Choudhary, K. K. Yadav, M. T. Qasim, R. Zairov, *et al.*, "Recent advances in the synthesis of nitrogen-containing heterocyclic compounds via multicomponent reaction and their emerging biological applications: A review," *Journal of the Iranian Chemical Society*, vol. 22, no. 1, pp. 1–33, 2025.

[2] A. Al-Mulla, "A review: Biological importance of heterocyclic compounds," *Der Pharma Chemica*, vol. 9, no. 13, pp. 141–147, 2017.

[3] J. Baranwal, S. Kushwaha, S. Singh, and A. Jyoti, "A review on the synthesis and pharmacological activity of heterocyclic compounds," *Current Physical Chemistry*, vol. 13, no. 1, pp. 2–19, 2023.

[4] M. M. Al-Tufah, "Synthesis and identification of novel 1,3-oxazepane-7,4-dione compounds via the reaction of succinic anhydride with Schiff's base and assessment of biological activity," *Central Asian Journal of Theoretical and Applied Science*, vol. 6, no. 1, pp. 34–51, 2025.

[5] C. Santhosh, S. Chinnam, S. J. Shivaram, V. T. Fernandes, K. Chidambaram, H. K. Prakash, S. Gadde, and G. M. Madhu, "Synthesis of pyrimidine-based analogues: A comprehensive review," *Journal of Chemical Reviews*, vol. 7, no. 4, pp. 591–634, 2025.

[6] V. Alagarsamy, B. Narendhar, M. T. Sulthana, G. Sabarees, and V. R. Solomon, "Pyrimidine-based scaffolds: Emerging frontiers in antimicrobial drug discovery," *ChemistrySelect*, vol. 10, no. 27, Art. no. e00907, 2025.

[7] N. R. Sutar, S. G. Alegaon, and G. A. Govind, "A detailed review of recent developments in the synthesis of pyrimidine derivatives and their anticancer potential," *IJSAT—International Journal on Science and Technology*, vol. 16, no. 2, 2025.

[8] S. Ali and J. Zhou, "Key contemporary considerations for halogens in drug discovery," Taylor & Francis, pp. 1–4, 2026.

[9] Z. Ma, S. Qiu, H.-C. Chen, D. Zhang, Y.-L. Lu, and X.-L. Chen, "Maleimide structure: A promising scaffold for the development of antimicrobial agents," *Journal of Asian Natural Products Research*, vol. 24, no. 1, pp. 1–14, 2022.

[10] O. I. Kalaoglu-Altan, R. Sanyal, and A. Sanyal, "Orthogonally 'clickable' biodegradable nanofibers: Tailoring biomaterials for specific protein immobilization," *ACS Omega*, vol. 4, no. 1, pp. 121–129, 2019.

[11] N. Kushwaha and D. Kaushik, "Recent advances and future prospects of phthalimide derivatives," *Journal of Applied Pharmaceutical Science*, vol. 6, no. 3, pp. 159–171, 2016.

[12] G. F. Fernandes, J. R. Lopes, J. L. Dos Santos, and C. B. Scarim, "Phthalimide as a versatile pharmacophore scaffold: Unlocking its diverse biological activities," *Drug Development Research*, vol. 84, no. 7, pp. 1346–1375, 2023.

[13] H. A. Sahib and M. H. Mohammed, "Synthesis and preliminary biological activity evaluation of new N-substituted phthalimide derivatives," *Iraqi Journal of Pharmaceutical Sciences*, vol. 29, no. 1, pp. 247–252, 2020.

[14] H. M. Heras Martinez, E. Barragan, K. O. Marichev, D. Chávez-Flores, and A. Bugarin, "Phthalimides as anti-inflammatory agents," *Future Medicinal Chemistry*, vol. 17, no. 1, pp. 125–142, 2025.

[15] H. Jelali, L. Mansour, E. Deniau, M. Sauthier, and N. Hamdi, "An efficient synthesis of phthalimides and their biological activities," *Polycyclic Aromatic Compounds*, vol. 42, no. 4, pp. 1806–1813, 2022.

[16] M. Kaur, S. Sharma, and D. Utreja, "A review on drug discovery of phthalimide analogues as emerging pharmacophores: Synthesis and biological potential," *ChemistrySelect*, vol. 10, no. 16, Art. no. e202405580, 2025.

[17] I. Silini, Z. Rouibah, H. Bouraoui, M. Ahmida, S. Nedjai, I. Grib, *et al.*, "Anti-oxidant and antibacterial activities of novel N-sulfonylphthalimide in an ovalbumin-induced inflammation in Wistar rats," *Cellular and Molecular Biology*, vol. 70, no. 9, pp. 114–120, 2024.

[18] H. A. Abuelizz, A. H. Bakheit, M. Marzouk, M. M. Abdellatif, and R. Al-Salahi, "Reactivity of 4,5-dichlorophthalic anhydride towards thiosemicarbazide and amines: Synthesis, spectroscopic analysis, and DFT study," *Molecules*, vol. 27, no. 11, Art. no. 3550, 2022.

[19] K. Al-Badrany, S. Jasim, and M. Al-Tufah, "Synthesis of some compounds of chalcones and pyrozoline containing phthalimide unit and evaluation of their biological activity," *Samarra Journal of Pure and Applied Science*, vol. 2, no. 4, 2020.

[20] D. R. Kashash, M. M. Kareem, and N. A. Naser, "New N-substituted maleimide homopolymers as drug carrier: Synthesis and biological activity," 2025.

[21] R. A. Pophale and M. N. Deodhar, "Synthesis and evaluation of novel phthalimide derivatives as analgesic and anti-inflammatory agents," *Der Pharma Chemica*, vol. 2, no. 1, pp. 185–193, 2010.

[22] M. M. Al-Tufah, S. S. Jasim, and K. A. Al-Badrany, "Synthesis and antibacterial evaluation of some new pyrazole derivatives," *Prof. (Dr.) R. K. Sharma*, vol. 20, no. 3, p. 178, 2020.

[23] N. M. Alassadi and M. K. Hadi, "Synthesis, characterization and preliminary antimicrobial study of some new phthalimide phenyl hydrazide derivatives," *F1000Research*, vol. 13, Art. no. 245, 2024.

[24] M. M. Al-Tufah, "Synthesis and identification of some new bi-azetidine-2,2′-dione and bi-quinazoline-4,4′-dione compounds derived from bis Schiff base derivatives," *Samarra Journal of Pure and Applied Science*, vol. 7, no. 2, pp. 56–76, 2025.

[25] D. Z. Mutlaq, A. A. Al-Shawi, and R. H. Al-Asadi, "Synthesis, characterization, anticancer activity, and molecular docking of novel maleimide–succinimide derivatives," *Egyptian Pharmaceutical Journal*, vol. 20, no. 4, pp. 303–312, 2021.

[26] K. J. Nelson, T. L. Smalley, Jr., T. Messier, R. Gumpena, U. Gandhi, S. Milczarek, *et al.*, "Mechanism-based peroxiredoxin 3 inhibitors exploit a covalent warhead for cancer therapy," *Science Advances*, vol. 11, no. 44, Art. no. eady4492, 2025.

[27] M. Sevindik, C. Bal, T. Krupodorova, A. Gürgen, and E. C. Eraslan, "Extract optimization and biological activities of *Otidea onotica* using artificial neural network-genetic algorithm and response surface methodology techniques," *BMC Biotechnology*, vol. 25, no. 1, Art. no. 25, 2025.

[28] F. A. Ahmed and D. Mutlaq, "Synthesis and anti-breast cancer activity of some succinimide derivatives via Michael addition reaction: Arylhydrazide to maleimides," *Journal of Basrah Researches (Sciences)*, vol. 50, no. 2, pp. 28–197, 2024.

[29] S. J. Faisal and D. Z. Mutlaq, "Synthesis, characterization and anti-breast cancer activity of some maleimide derivatives," *Al-Kufa University Journal for Biology*, vol. 14, no. 3, pp. 83–102, 2022.

[30] J. Wang, Y. Zhang, B. Wang, Y. Xia, F. Xue, W. Jin, *et al.*, "Electrooxidative Hofmann rearrangement of phthalimides to access anthranilate derivatives," *ACS Omega*, vol. 8, no. 38, p. 35167, 2023.

[31] S. Kotowicz, J. G. Małecki, J. Cytarska, A. Baranowska-Łączkowska, M. Siwy, K. Z. Łączkowski, *et al.*, "Effect of N-phenyl substituent on thermal, optical, electrochemical and luminescence properties of 3-aminophthalimide derivatives," *Scientific Reports*, vol. 13, no. 1, Art. no. 19801, 2023.

[32] A. Mahmoudi and S. Francia, "Comparative analysis and application of novel spectrophotometric approaches and bioassay for fast macrolide quantification in table," *Chemistry Journal of Moldova*, vol. 20, no. 1, pp. 7–16, 2025.

[33] R. Neagu, V. Popovici, L.-E. Ionescu, V. Ordeanu, A. Biță, D. M. Popescu, *et al.*, "Phytochemical screening and antibacterial activity of commercially available essential oils combinations with conventional antibiotics against gram-positive and gram-negative bacteria," *Antibiotics*, vol. 13, no. 6, Art. no. 478, 2024.